

Supporting Information for Can Large-Scale Clustering of Tropical Precipitation Be Used to Constrain Climate Sensitivity?

P. Blackberg^{1,2}, M. S. Singh^{1,2}

¹School of Earth, Atmosphere, and Environment, Monash University, Victoria, Australia

²Centre of Excellence for the Weather of the 21st Century, Monash University, Victoria, Australia

Contents of this file

1. Figures S1 to S8
2. Tables S1 to S2

Corresponding author: P. Blackberg, carlphiliposcar@gmail.com

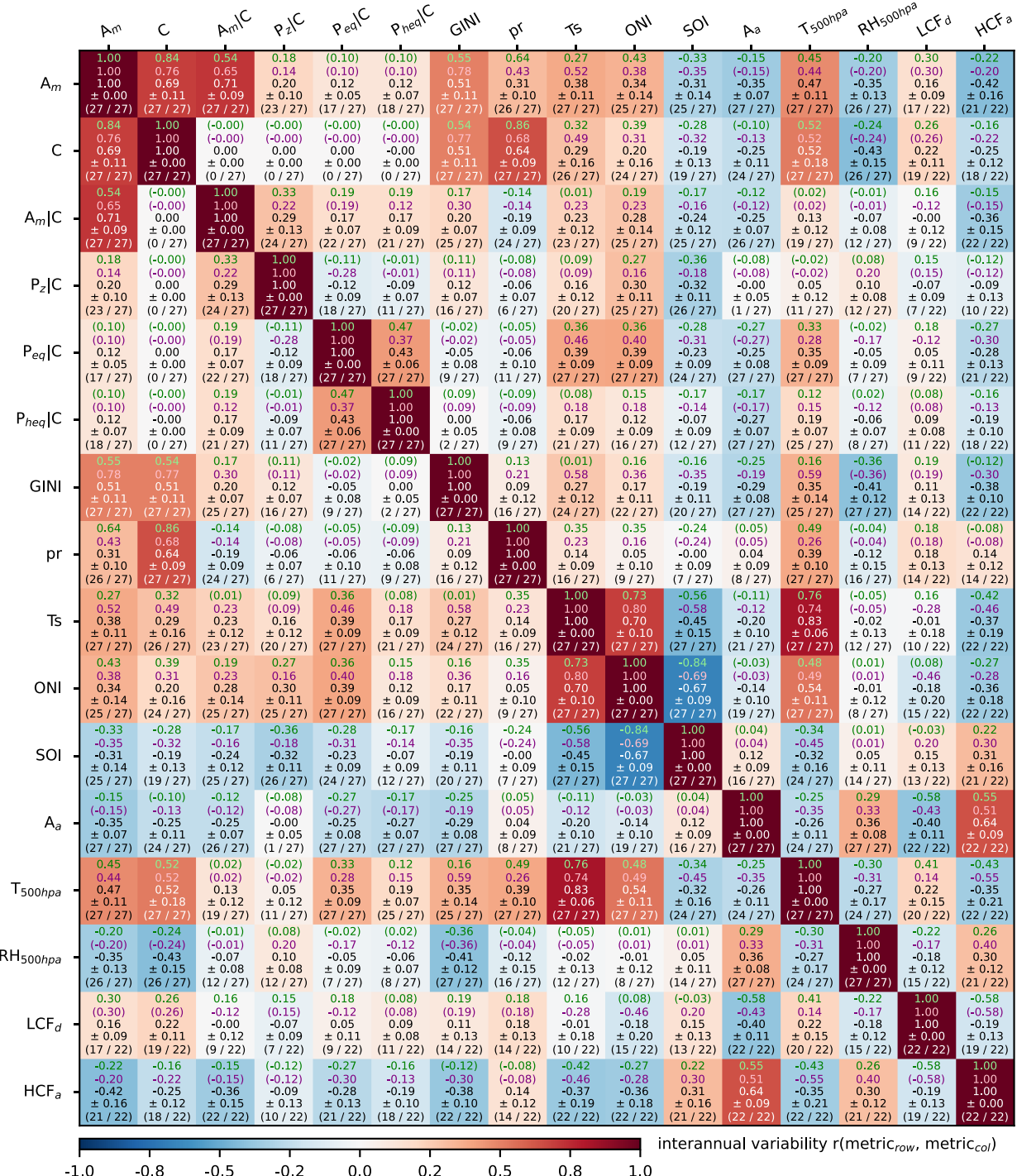


Figure S1. Correlation matrix for interannual variability, in observations (green), IFS_9-FESOM_5 (purple), and the CMIP ensemble mean and standard deviation (black). The colors represent the sign and strength of the correlations from the observations. Numbers in brackets are not statistically significant from zero, and the fraction in brackets show the number of models with statistically significant correlations. Details of the metrics are given in Table S2.

January 12, 2026, 4:03pm

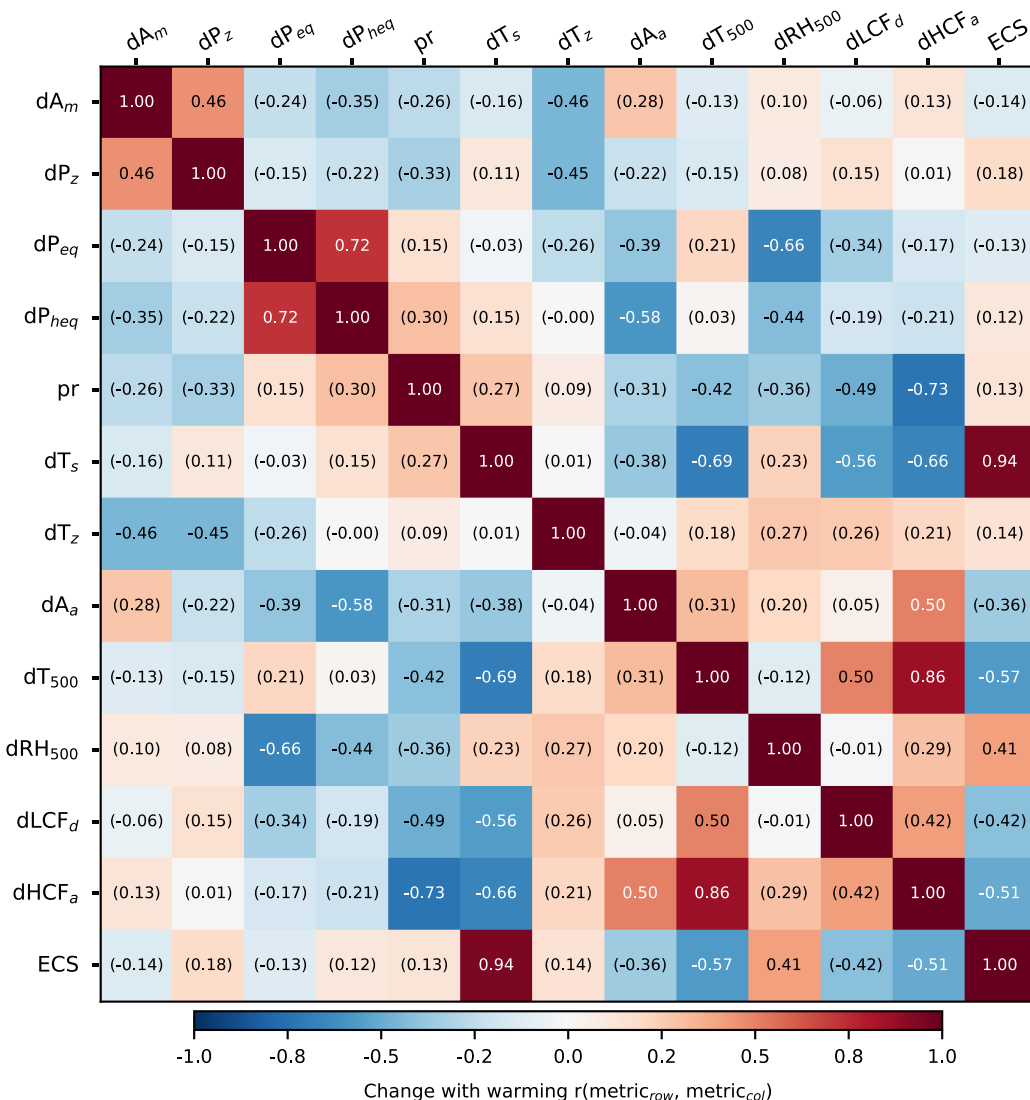


Figure S2. Correlation matrix for climatological change with warming across the CMIP6 ensemble. All metrics are normalized by the change in tropical-mean temperature (land and ocean) except for tropical-mean temperature itself and ECS. Numbers in brackets are not statistically different from zero.

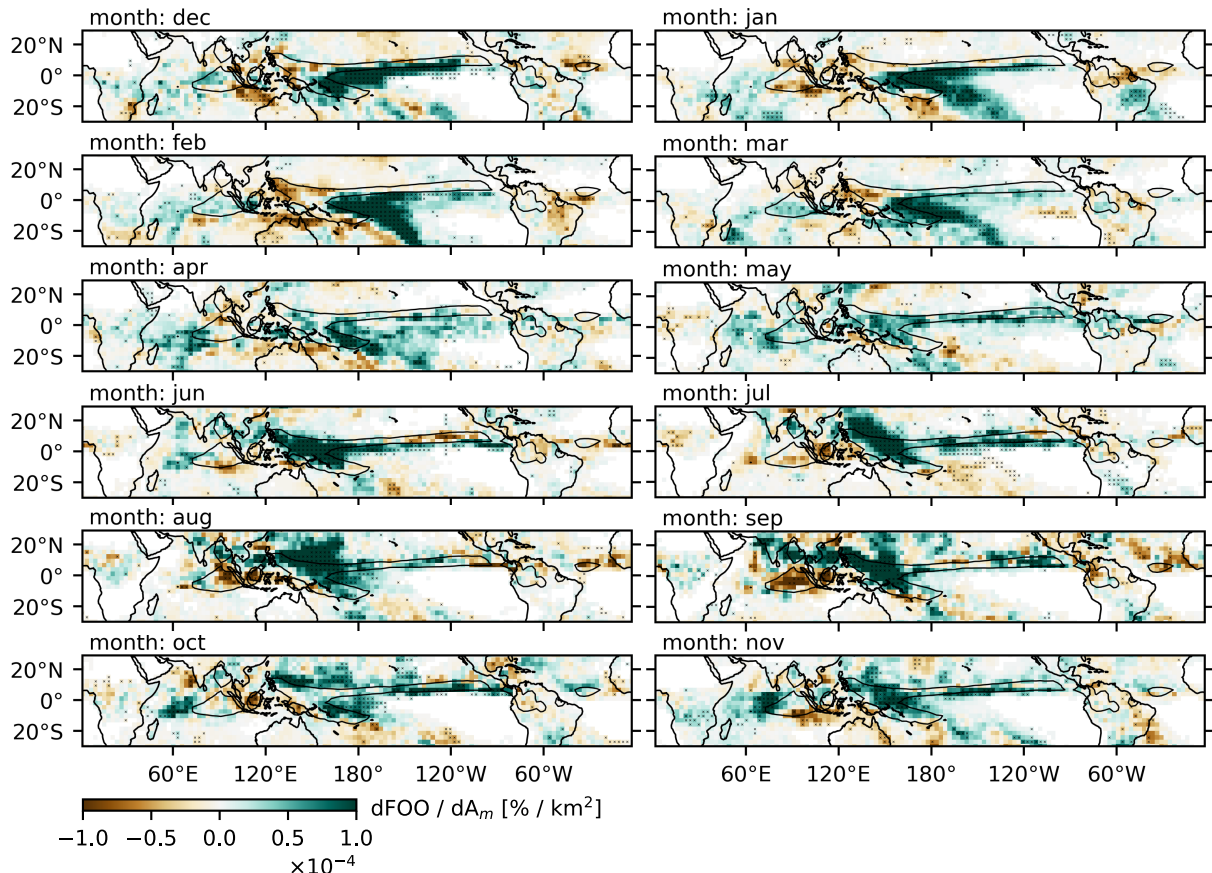


Figure S3. GPCP Frequency of occurrence of heavy precipitation, FOO , regressed onto the mean area of heavy precipitation features, A_m , for each month. Crosses indicate whether correlations are statistically significant.

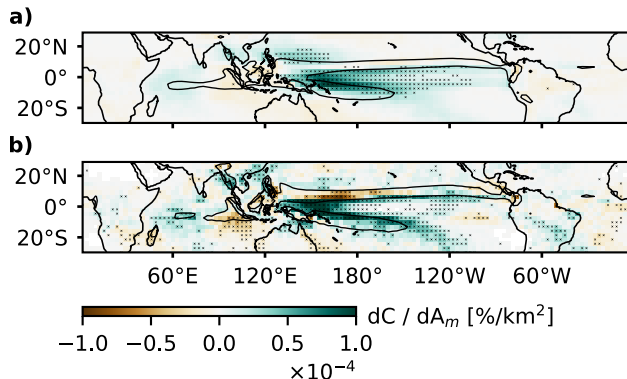


Figure S4. Frequency of occurrence of heavy precipitation, FOO , regressed onto the mean area of heavy precipitation features, A_m , in interannual variability for the CMIP ensemble-mean, (a) and IFS_9_FESOM_5 (b). The contour shows the 90th percentile of the climatological FOO and crosses indicate whether correlations are statistically significant.

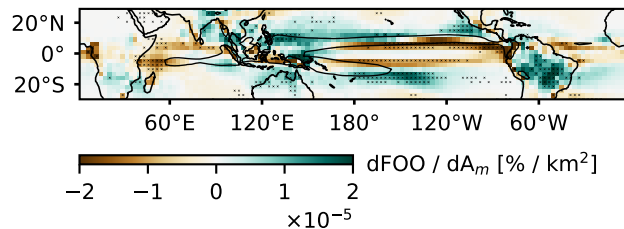


Figure S5. Frequency of occurrence of heavy precipitation, FOO , regressed onto the mean area of heavy precipitation features, A_m , across the CMIP ensemble in climatological values. The contour shows the ensemble-mean 90th percentile of the climatological FOO and crosses indicate whether correlations are statistically significant.

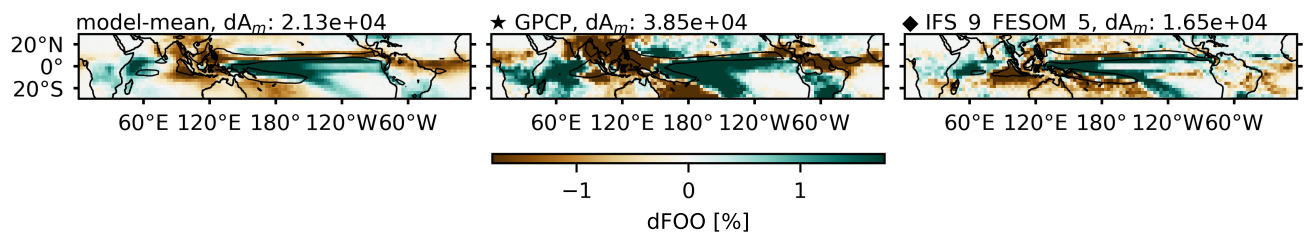


Figure S6. Difference in frequency of occurrence of heavy precipitation, FOO , during El Niño events and during all days in the CMIP6 ensemble-mean, in observations: GPCP, and for the high-resolution model: IFS_9_FESOM_5.

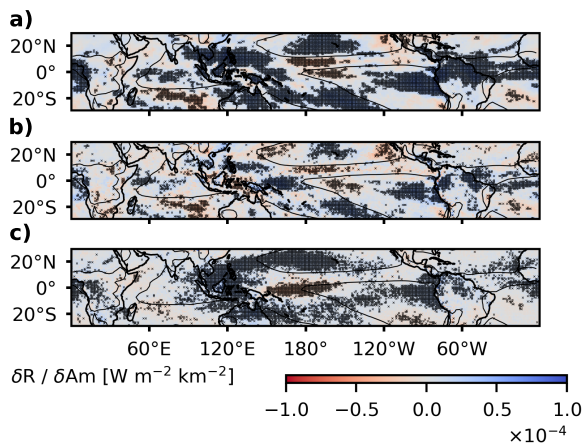


Figure S7. CERES-SYN1deg top of the atmosphere net radiative fluxes for all (a), cloud-radiative (b), and clear-sky (c) conditions regressed onto mean area of heavy precipitation features, A_m . Crosses indicate whether correlations are statistically significant.

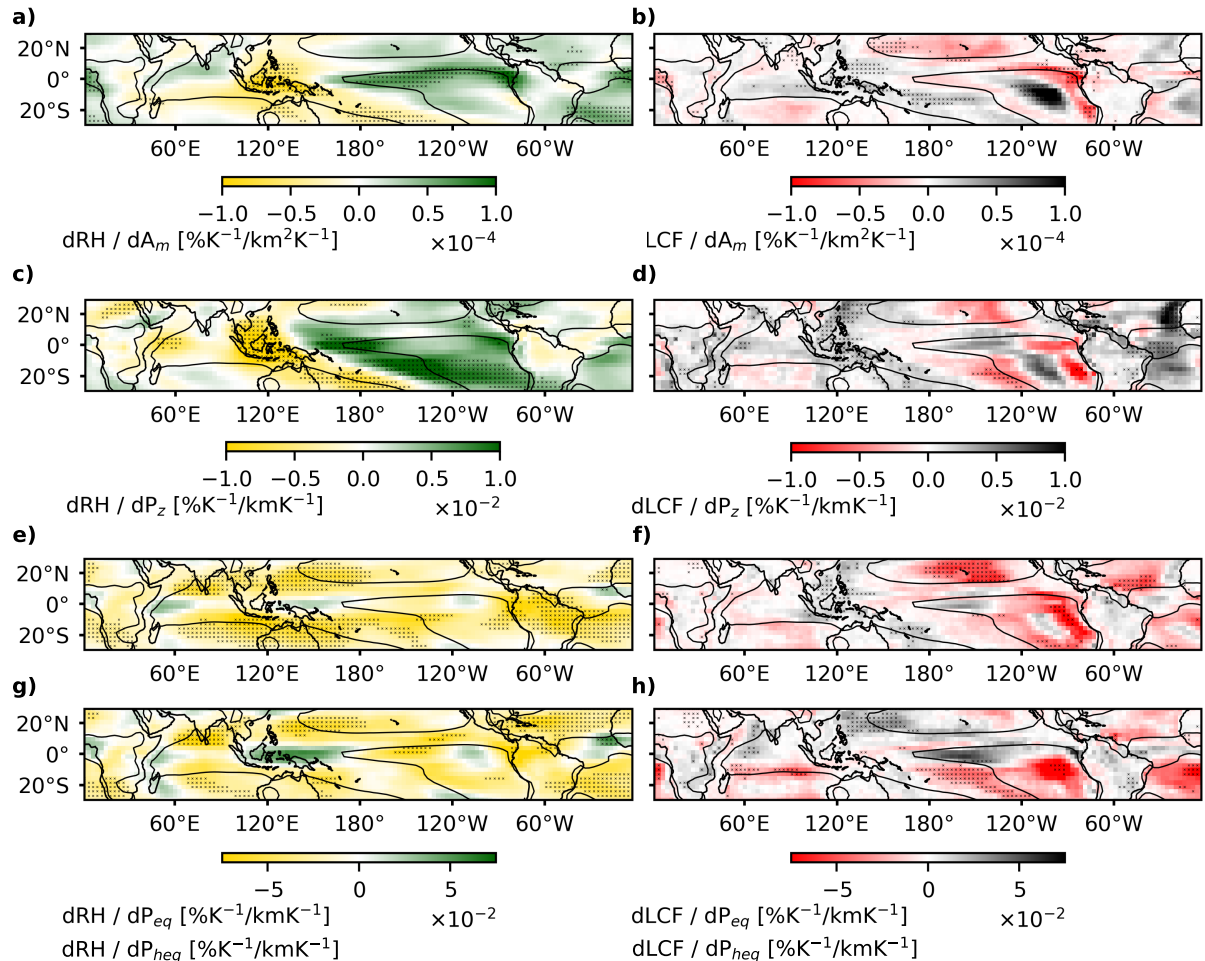


Figure S8. Change in relative humidity (RH, left) and low cloud fraction (LCF, right) regressed onto; A_m (a-b), P_z (c-d), P_{eq} (e-f), and P_{heq} (g-h) per Kelvin warming across the CMIP ensemble.

Table S1. Models from the CMIP6 archive that were used in this study.

Institute	Model	Ensemble
INM	INM-CM5-0	r1i1p1f1
CCCR-IITM	IITM-ESM	r1i1p1f1
CAS	FGOALS-g3	r1i1p1f1
INM	INM-CM4-8	r1i1p1f1
MIROC	MIROC6	r1i1p1f1
MPI-M	MPI-ESM1-2-LR	r1i1p1f1
BCC	BCC-CSM2-MR	r1i1p1f1
NOAA-GFDL	GFDL-ESM4	r1i1p1f1
MIROC	MIROC-ES2L	r1i1p1f2
NorESM2-LM	NCC	r1i1p1f1
MRI	MRI-ESM2-0	r1i1p1f1
NOAA-GFDL	GFDL-CM4	r1i1p1f1
CMCC	CMCC-CM2-SR5	r1i1p1f1
CMCC	CMCC-ESM2	r1i1p1f1
NUIST	NESM3	r1i1p1f1
CSIRO	ACCESS-ESM1-5	r1i1p1f1
CNRM-CERFACS	CNRM-ESM2-1	r1i1p1f2
EC-Earth-Consortium	EC-Earth3	r1i1p1f1
CNRM-CERFACS	CNRM-CM6-1	r1i1p1f2
CNRM-CERFACS	CNRM-CM6-1-HR	r1i1p1f2
NIMS-KMA	KACE-1-0-G	r1i1p1f1
IPSL	IPSL-CM6A-LR	r1i1p1f1
CSIRO-ARCCSS	ACCESS-CM2	r1i1p1f1
AS-RCEC	TaiESM1	r1i1p1f1
NCAR	CESM2-WACCM	r1i1p1f1
CCCma	CanESM5	r1i1p1f1
MOHC	UKESM1-0-LL	r1i1p1f2

Table S2. Metrics used in this study.

Metric	description
A_m	Mean area of heavy precipitation features.
A_f	Total area of heavy precipitation features.
$A_m C$	Spatial clustering from changes in mean area, independent of total area coverage ($A_m C = A_m - \alpha C$), where α is a constant.
P_z	Mean distance of heavy precipitation points to the meridian given by the longitude 180°E.
P_{eq}	Mean distance of heavy precipitation points to the geographic equator.
P_{heq}	Mean distance of heavy precipitation points to the hydrological equator, where the hydrological equator is defined as the latitude of highest specific humidity at 700 hPa as a function of longitude for the associated month.
<i>GINI</i>	Relative dispersion measure of the precipitation field, quantifying the "unevenness" of the distribution normalized by the mean (GINI; Gini, 1912).
T_s	Tropical-mean 2m air temperature.
T_{500hpa}	Tropical-mean temperature at 500 hPa.
<i>ONI</i>	Three-month rolling average SST anomaly in the Niño3.4 region (5°S- 5°N, 120°-170°W), relative to the full range of years used in the climatology.
<i>SOI</i>	standardized deseasonalized monthly anomalies of the surface pressure difference between Tahiti (17.6°S, 149.6°W) and Darwin (12.5°S, 130.9°E), calculated here as the three-month rolling average.
LCF_d	Tropical-mean low-cloud fraction, in regions where the monthly-mean vertical pressure velocity at 500 hPa is positive (in regions of descent).
RH_{500hpa}	Tropical-mean relative humidity at 500 hPa.
HCF_a	Tropical-mean high-cloud fraction, in regions where the monthly-mean vertical pressure velocity at 500 hPa is negative (in regions of ascent).
A_a	Area where the monthly-mean vertical pressure velocity at 500 hPa is negative, as a fraction of the tropical domain area (area of ascent).
<i>ECS</i>	Equilibrium Climate Sensitivity.